Modeling of Platinum-Aryl Interaction with Amyloid-β Peptide

Matthew Turner[1] James A. Platts[1] and Robert J. Deeth[2†]*

[1] School of Chemistry, Cardiff University, Park Place, Cardiff CF10 3AT, UK; [2] Department of Chemistry, University of Warwick, Gibbet Hill, Coventry, CV4 7AL

Abstract

Ligand field molecular mechanics (LFMM), density functional theory (DFT) and semi-empirical PM7 methods are used to study the binding of two Pt(II)-L systems to an N-terminal fragment of the amyloid-β peptide, where L = 2,2-bipyridyl or 1,10-phenanthroline. Molecular dynamics simulations are used to explore the conformational freedom of the peptide using LFMM combined with AMBER molecular mechanics parameters. We establish a modelling protocol, allowing for identification and analysis of favorable platinum-binding modes and peptide conformations. Preferred binding modes are identified for each ligand investigated; metal coordination occurs via Nε in His residues for both ligands - His6ε-His13ε and His6ε-His14ε for the bipyridyl and phenanthroline ligands, respectively. The observed change in binding mode for the different ligands suggests that the binding mode of these platinum-based structures can be controlled by the choice of ligand. In the bipy systems, Boltzmann population at 310K is dominated by a single conformer, while in the phenanthroline case, three conformations make significant contributions

to the ensemble. The relative stability of these conformations is due to the inherent stability of binding platinum via Nε in addition to subtle H-bonding effects.

Introduction

Alzheimer's disease (AD) is a widespread neurodegenerative condition associated with progressive cognitive decline in patients. AD is the most common cause of dementia in adults and the fourth most common cause of death in Western countries.[1] The pathogenesis of AD is complex, involving the interplay of a range of molecular, cellular and physiological processes[2]; the causes and development of AD are not well understood, with links to both lifestyle[3,4] and genealogy.[5] Amyloid-β (Aβ) peptide was first recognized as a factor in AD in 1985[6] and has been the subject of the much research in the decades since. The well-publicized amyloid-cascade hypothesis remains popular, if controversial, and suggests that individual Aβ peptides - between 39-43 residues in length - agglomerate, leading to plaque formation.[7,8,9,10] These plaques are thought to be the cause of local inflammation and neuronal cell death. Subsequent effects seen in AD may be caused by this imbalance between Aβ generation and clearance. As such, the early stages of Aβ aggregation form a realistic druggable target for the development of anti-AD therapeutics.[2]

The N-terminal region of Aβ contains histidine-rich metal binding sites that are responsible for physiological coordination of transition metals. These metal ions are believed to play an important role in the development of amyloid plaques; analysis of fibrils in Alzheimer's brains proves that they show increased concentrations of transition metal ions such as Cu, Zn and Fe.[11,12] However, the exact metal binding sites are the subject of debate, with authors showing varied metal coordination involving several different peptide residues, though N-terminal histidines at positions 6, 13 and 14 feature prominently.[13,14,15,16] One route to potential therapeutic agents for AD is the

development of compounds that selectively occupy Cu/Zn binding sites on Aβ and so prevent aggregation and oligomerisation.

Pioneering work by Barnham *et al*.[17] showed that Pt^{II}(phenanthroline) complexes are able to inhibit Aβ aggregation, and inhibit its neurotoxicity *in vitro*. Additionally, Pt(II) compounds are stable (*i.e.* kinetically and redox inert) in biological systems, meaning that once the Pt(II) complex is bound to a target, it is very difficult to displace. However, there has been a great deal of debate over exactly how these platinum-ligand systems interact with the Aβ peptide. Of particular relevance to the current study, Streltsov *et al* combined DFT and EXAFS data for a Pt(phen)$(imidazole)_2$ model complex to arrive at experimentally derived predictions of binding modes.[18]

Spectroscopic evidence[19] suggests that several platinum adducts are formed in the coordination of Pt^{II}(phen) complexes to Aβ, but that His-6 and His-14 are preferentially bound. Recent work has also shown that aromatic ligands such an phenanthroline are vital for activity - it is believed that π-π stacking interactions between the ligands and aromatic residues Phe, Tyr and His are important in the association of Pt^{II}(phen) to Aβ.[17,20,21]

Computational modelling of molecules of this type present significant challenges; quantum mechanical (QM) methods such as DFT are not routinely applicable to large protein systems, especially flexible ones such as Aβ. Classical modelling techniques using molecular mechanics (MM) forcefields typically fail to model the effects of transition metal d-electrons on the structure and properties of coordination complexes. This problem may be circumvented by combining the quantum and classical techniques, using QM for the metal center and MM for the remainder of the system. This QM/MM approach is widely used and has been applied to metal-biomolecule systems

similar to those investigated here[22,23,24]. However, there is still a significant cost associated with the QM calculation compared to pure MM.

An alternative is ligand field molecular mechanics (LFMM)[25,26], designed to provide '*the flexibility and generality of quantum mechanics with the speed of molecular mechanics.*'[26] This technique has been applied to the study of a variety of complex metal-based systems, such as d^9 Cu(II)[27], high- and low-spin d^8 Ni(II)[28] and d^8 Pt(II)[29,30]. The aim of this work is to establish a protocol for generating and subsequently analyzing conformations of a series of platinum(II) species bound to a fragment of Aβ peptide (residues 6-14 – see Figure 1), with the aim of identifying favorable metal-binding modes and peptide conformations. This model is too small to truly represent the biology of Aβ, but this subset of residues is large enough to contain those important for platinum binding, while remaining such a size that we can benchmark computational results against DFT. This preliminary work presents findings for two platinum-ligand systems: 2,2-bipyridyl (bipy) and 1,10-phenanthroline (phen), the choice of which stem from recent literature. Ultimately, this protocol could be extended to study other ligands, different transition metals such as those of physiological importance (*e.g.* copper and zinc)[31] or other potential therapeutics of current research interest (*e.g.* ruthenium)[32].

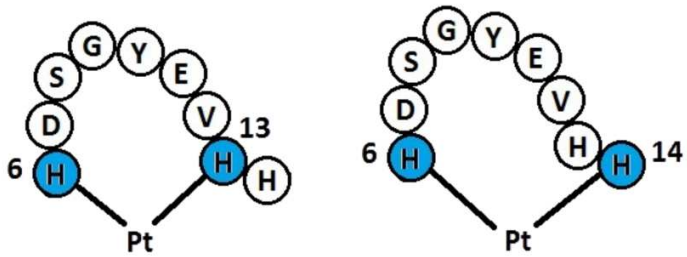

Figure 1. Schematic of PtL (L = bipy or phen) binding to residues 6-14 of Aβ peptide

Computational Methods

The peptide sequence His6-Asp-Ser-Gly-Tyr-Glu-Val-His-His14, taken from the N-terminal domain of Aβ was built in an extended conformation in MOE[33]. Pt was added in eight distinct coordination modes (*i.e.* to His6 and either His13 or His14 through Nδ or Nε), and the bipyridine or phenanthroline ligand manually constructed. For conformational searching, the resulting complexes were described using molecular mechanics using a combination of ligand field molecular mechanics (LFMM) for Pt[26,29,30] and AMBER94[34] parameters for all other atoms, as implemented in the DommiMOE[35] extension to MOE. Partial charges for Pt and coordinated groups were calculated for model Pt(imidazole)$_2$(ligand) systems using the Merz-Kollman scheme from HF/6-31G(d)/SDD electrostatic potential in Gaussian09[36], with Pt given a van der Waals radius of 2.0 Å. The remaining peptide atoms, *i.e.* those beyond coordinated imidazole, were given AMBER94 charges as calculated by MOE. Solvation effects were modelled using the reaction-field model with default parameters.

Conformational freedom was explored through the LowMode MD[37] method in MOE. LowMode MD searches were configured to terminate after 100 successive failures to generate a new molecular conformation, up to a maximum of 10,000 iterations. An arbitrarily large energy cut-off (10,000 kcalmol^{-1}) was used alongside an RMSD cut-off of 0.25 Å for retention of all new conformations. LowMode MD is able to analyze complex molecular systems such as protein loops and macrocycles, taking into account complex non-bonded interactions, and is able to locate low-energy conformations for a variety of structures in a computationally efficient manner[37,38,39]. During initial conformational searches, it was found that often a large portion of the kinetic energy was localized on the four Pt-N coordination bonds. These bonds are not important for exploring

conformations since their final position is determined by the LFSE contribution to LFMM. This lead to the LowMode MD search becoming 'stuck' and unable to escape a certain conformation, resulting in the premature termination of the conformational search. We resolved this by fixing the platinum centre, making the mass of this atom effectively infinite.

DFT calculations were performed using Gaussian09 with the BHandH[40] functional with a 6-31G(d) basis set on all atoms in conjunction with a Stuttgart-Dresden (SDD)[41,42] effective core potential for platinum(II), within a polarizable continuum model (PCM) model of aqueous solvation[43,44]. The choice of functional was determined by modelling relevant Pt(II) crystal structures, while BHandH has been widely used in description of π-stacking and other dispersion-based interactions.[45] In addition, two more modern functionals, B97D and M06-2X,[46,47] specifically designed to account for dispersion were tested for a subset of complexes. Semi-empirical calculations were performed using MOPAC[48] with the PM7 method[49] and the COSMO model of aqueous solvation[50]; full relaxation was achieved through use of keywords LET and DDMIN=0. Overlay plots were obtained using Chimera imaging software[51]. RMSD values were calculated using a python script obtained via GitHub (https://github.com/charnley/rmsd)[52,53].

Results and Discussion

Using the conformational searching protocol described above, searches were performed on the eight platinum binding modes of interest for each ligand system. This produced between 400 and 1600 conformers for each platinum binding mode (

Table **1**). There is appreciable variation between sets which may be at least partially due to the stochastic nature of the LowMode MD method as well as the inherent flexibility of the different complexes. For comparison, an identical simulation of the peptide fragment without Pt-

coordination results in 9,962 conformations from 10,000 starting attempts. It is therefore apparent from

Table **1** that Pt binding to two His residues allows the peptide chain significant flexibility, no matter which coordination mode is considered, but that this conformational freedom is significantly reduced compared to the free peptide.

Table 1. Number of conformers found using LowMode MD for the ligands studied.

Coordination mode	**bipy**	**phen**
6δ - 13δ	893	425
6δ - 13ε	426	495
6ε - 13δ	484	468
6ε - 13ε	995	405
6δ -14δ	574	411
6δ -14ε	1570	454
6ε - 14δ	429	618
6ε - 14ε	1135	450

While the MM protocol used to generate data in

Table **1** has been successfully applied to many similar problems, it is important to validate the results it provides against other theoretical approaches. In particular, we note that LFMM has long-standing use for metal-peptide binding, but that Pt(II) is not yet among the metals used. Pt(II) parameters are available, and have been used to model Pt-DNA complexes[29,30]. In the current case, the relatively flexible peptide fragment contrasts with more structured protein and DNA for which

LFMM has typically been used. DFT was therefore applied to a subset of 158 unique low-energy conformers, encompassing several different platinum-binding modes, in order to test further computational methods. We first consider the relative energies of LFMM-generated structures, calculated without further geometry relaxation. We find little correlation between LFMM and DFT relative energies at LFMM geometry ($R^2 = 0.14$), suggesting that the combined LFMM/AMBER approach does not accurately predict the relative energies of different conformers.

In order to check the reliability of DFT methods used as a benchmark, a set of non-platinated conformations was constructed by removing PtL from conformations located as discussed above, and their energies calculated using DFT and AMBER. Three different DFT methods (BHandH, B97D and M06-2X) show excellent agreement with one another (R^2 BHandH vs. B97D = 0.94, BHandH vs. M06-2X 0.93, B97D vs. M06-2X 0.95), supporting our conclusion that BHandH is a suitable method for these structures. Furthermore, these DFT methods show little agreement with the AMBER energies for these non-platinated systems (R^2 BHandH vs. AMBER = -0.02). This suggests that the poor agreement between DFT and LFMM/AMBER energies described above stems from the use of AMBER94 for the peptide, rather than from use of LFMM for the metal centre.

Due to the high computational expense of DFT calculations, a faster computational method was required to identify conformers of interest. PM7 and DFT energies of platinated conformations at MM geometries are in good agreement with one another ($R^2 = 0.78$); PM7 therefore reproduces DFT energies at a much lower computational cost. This suggests that PM7 is a suitable theoretical method for structures of this type. This assertion is reinforced by the modelling of the non-platinated conformations: BHandH and PM7 calculations show strong agreement ($R^2 = 0.77$), further showing that PM7 is an accurate and reliable alternative to DFT.

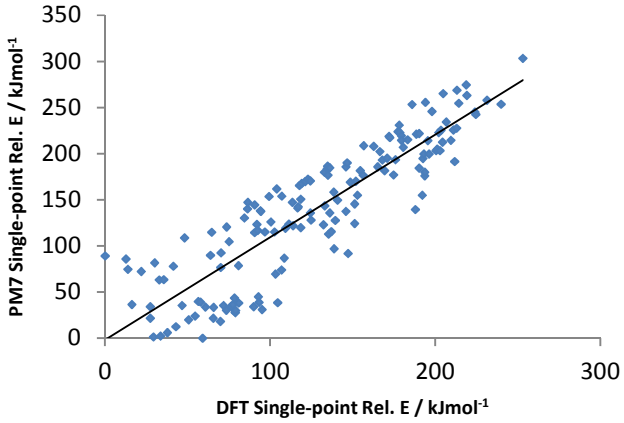

Figure 2. Plot of DFT vs. PM7 relative energies at LFMM geometry.

Table 2. Correlation between relative energies of 158 conformers.

	LFMM	**PM7**	**DFT**
LFMM	1.00	0.38	0.14
PM7	-	1.00	0.78
DFT	-	-	1.00

The other key consideration of the LFMM results is whether the geometries produced are reliable. We therefore carried out DFT and PM7 geometry optimization of all 158 platinated conformers, and evaluated the all-atom RMSD of the resulting structures from those obtained from LFMM energy minimization.

Table **3** reports the results of such comparison, and demonstrates that LFMM and DFT are in good general agreement, *i.e.* DFT optimization of a selected structure does not significantly alter the overall geometry, indicating that LFMM produces robust geometries.

Table 3. Summary of geometry comparison between LFMM, PM7 and DFT.

RMSD VALUES	**LFMM vs. DFT**	**PM7 vs. DFT**
Mean	0.670	0.817
SD	0.191	0.307
Min.	0.336	0.339
Max.	1.293	1.982

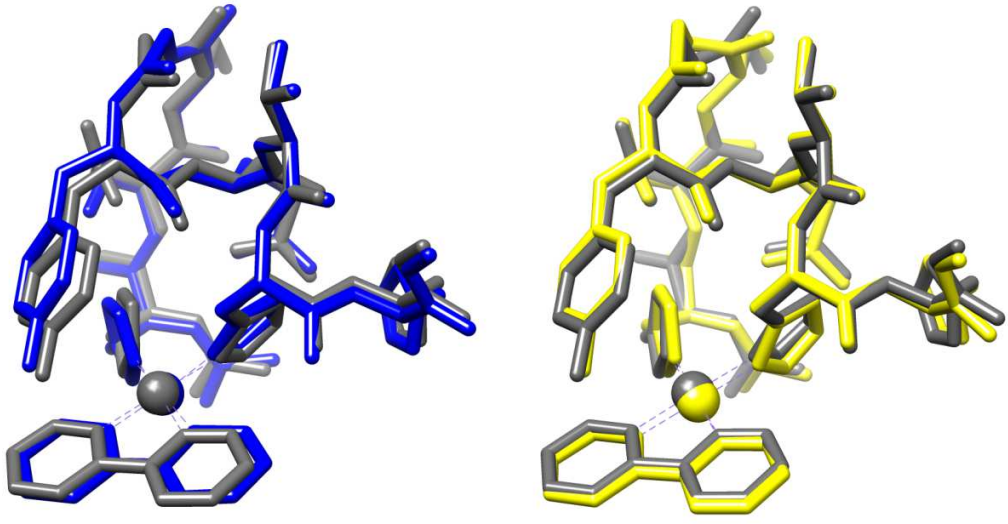

Figure 3. Left: LFMM (blue) vs DFT (grey) geometry overlay. Right: PM7 (yellow) vs DFT geometry (grey) overlay.

DFT optimization is a laborious task, requiring several CPU-weeks per structure on the computing resources available to us. We therefore also investigated whether the much faster PM7

approach might be suitable for this purpose. Table 3 shows that, on average, PM7-optimised structures are slightly further from DFT ones than LFMM structures (mean RMSD 0.82 vs. 0.67 Å). These values include data from 9 conformers for which PM7 predicts large (> 1.3 Å) RMSD from DFT-optimized geometry. For the remaining 149 structures, the mean RMSD is 0.77 Å. Interestingly, further DFT optimization for the 9 complexes with large RMSD, starting from the PM7 endpoint produced significant reduction in energy, indicating that in some cases PM7 geometry optimization in MOPAC is able to escape from the local minimum located by LFMM conformational search. One such case is illustrated in Figure 4 below, in which DFT optimization following initial PM7 refinement leads to a structure that is 62.3 kJ mol^{-1} more stable than that reached by optimization directly from the LFMM structure.

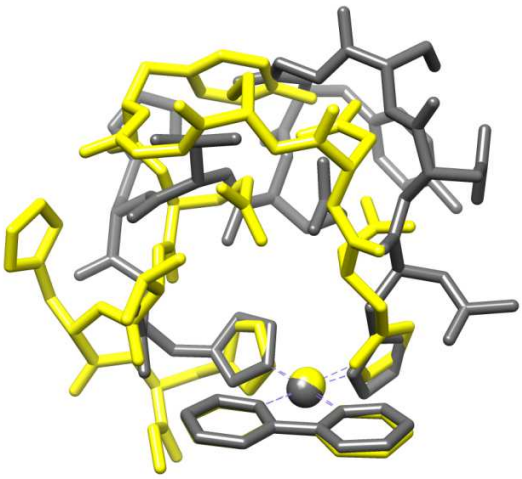

Figure 4. DFT optimised structure (grey) overlaid with PM7-DFT optimised structure (yellow).

We therefore surmise that PM7/COSMO optimization following initial LFMM conformational search is a useful step in obtaining reliable energy and geometry data. Although the extra step requires significant additional computational effort (PM7 optimization takes approximately 20

minutes per structure on a single compute node), the evidence above indicates that it provides a more balanced set of data than either LFMM alone or PM7 at the LFMM geometry. We therefore performed this step for all conformations located for both ligands, a total of 6506 for bipy and 3726 for phen. The resulting relative energies were collated and used in Boltzmann weighting to determine the binding mode(s) and conformation(s) that contribute significantly to the overall ensemble at 310 K, the results of which are reported in Table 4.

Table 4. Relative energy and Boltzmann factors for low energy conformations.

Ligand	**Coordination**	**Rel. E / kJ mol-1**	**Boltzmann fraction**
Bipy	6ε - 13ε	0.00	0.79
	“	6.27	0.07
	“	7.07	0.05
	“	7.51	0.04
Phen	6ε - 14ε	0.00	0.38
	“	0.77	0.28
	“	1.96	0.18
	“	4.14	0.08
	“	4.38	0.07

On the basis of these results, we predict that Pt(II) binds to histidine residues via Nε rather than Nδ. The first conformations that feature binding via Nδ of any His residue are found over 22 and 15 kJ mol^{-1} for bipy and phen ligands, respectively, and so contribute almost nothing to the Boltzmann-weighted ensemble of structures. This is an inherent property of the histidyl residue: calculations on a model system Pt(bipy)(Cl)His gives a preference for Nε over Nδ of 5 kJ mol^{-1} using DFT, and 3 kJ mol^{-1} using PM7. The data in Table 4 indicate that, out of the several thousand conformations considered, just a small number contribute significantly to the Boltzmann-weighted ensemble. A single conformation accounts for almost 80% of the ensemble of bipy complexes, and four conformations for over 95%. Three low energy conformations account for over 80% of the ensemble of phen complexes, and five account for 99%. This shows that coordination of Pt massively reduces the conformational freedom of the peptide by "pinning" two histidines to the metal center.

There is also a clear preference in coordination mode for each ligand; metal binding occurs via Nε of His-6 and His-13 for the bipy systems and via Nε of His-6 and His-14 for the phenanthroline systems. This result is particularly promising for the phenanthroline case, since the preferred metal-binding mode identified here (6ε - 14ε) was also determined to be the binding mode of this ligand system in experimental work carried out by Ma *et al*.[19] The fact that a relatively small change in ligand from bipy to phen alters the preferred coordination mode is somewhat surprising, and suggests that binding mode can be controlled through suitable choice of ligand.

To probe this change of binding mode in more detail,

Table **5** reports selected details of the DFT-optimized structures of the low energy conformation(s) for each ligand system. These data show that there is almost no variation in Pt—N bond lengths following change in conformation and/or coordinated ligand. In the bipy complex, the bonds to the N-donor ligands are slightly longer than those to the histidine residues of Aβ (mean values 1.963±0.004 vs 1.986±0.000 Å). Moreover, Pt—N_{His} distances are slightly shorter in the low energy bipy conformation than the average over all conformations located for the same binding mode (mean = 1.966 Å ±0.005), whereas Pt—N_{Lig} distances are slightly larger (mean = 1.981 Å ± 0.004). However, differences are typically within 1 or 2 standard deviations, and so not statistically significant. One apparently significant difference lies in the N_{His}-Pt-N_{His} angle that is on average 84.5° (±1.75) for the collection of 6ε - 13ε conformations but 88.5° in the single low-energy conformation. It is notable that these Pt—N distances are in good agreement with those reported by Streltsov *et al*,[18] Pt–N(imidazole) and Pt–N(phen) bond distances of 1.99(1) Å and 1.993(5) Å, respectively.

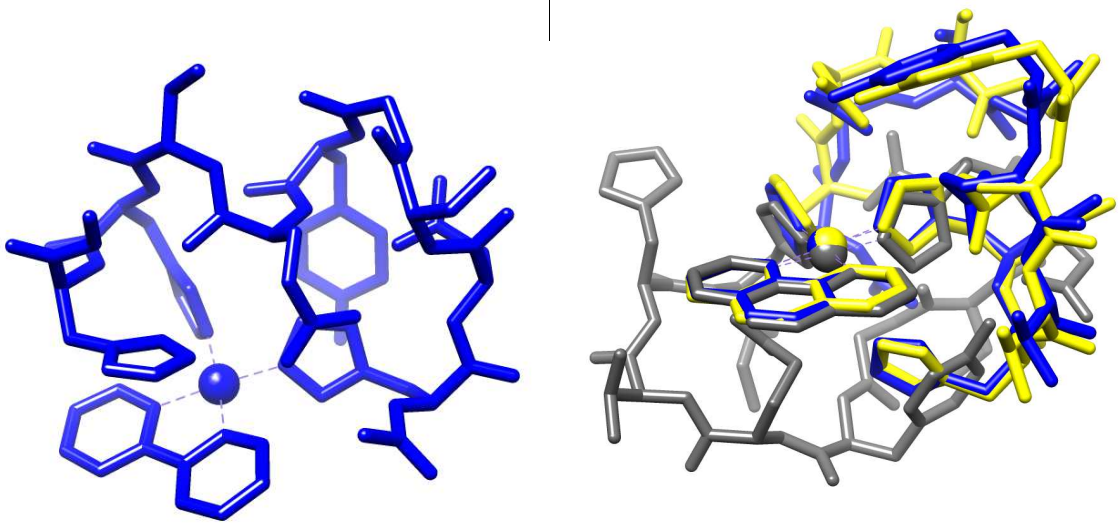

Figure 5. Left: Low energy bipy conformation. Right: Lowest (grey), second- and third-lowest (yellow and blue, respectively) conformations of phen system.

Table 5. Selected geometrical details of single low energy conformations (Pt-bipy) and three low energy conformations (Pt-Phen)

Structure	Pt-N_{His}	Pt-N_{Lig}	N_{His}-Pt-N_{His}	N_{Lig}-Pt-N_{Lig}	H-bonds	π-π
Pt-bipy	1.960	1.986	88.5	80.9	14	1
	1.966	1.986				
Pt-phen 1	1.958	1.994	85.2	82.1	12	0
	1.961	1.989				
2	1.964	1.994	83.1	81.8	7	0
	1.966	1.993				
3	1.961	1.992	82.8	81.6	6	0
	1.976	1.995				

As expected for biomolecular systems, a large number of intramolecular hydrogen bonds are present in the low energy conformations, including backbone-backbone, backbone-side chain and side chain-side chain interactions. The low energy Pt-bipy complex contains 14 H-bonds, as judged by geometrical criteria. Of these, five are concentrated around Glu-11 and a further three around Asp7. Four of these H-bonds are relatively long at over 2 Å, but a number of strong interactions were also identified, including those between backbone and residue (Asp7 – backbone N-H at 1.659 Å and Glu11 – N-terminal N-H at 1.794 Å) and residue-residue (Glu11 – His14 at 1.691 Å and Asp7 – His13 at 1.775 Å) which may be responsible for the stability of this conformation. In addition, four backbone-backbone H-bonds were identified in residues Gly9-His14. The low energy bipy conformation also contains a possible π–π interaction between bipy and the imidazole

side chain of His14. The two ring systems lie in an approximately parallel orientation (angle between mean planes = 29.9°) with an inter-centroid distance of approximately 4 Å.

The Pt-phen complexes identified exhibit markedly fewer H-bonds than the bipy complex, and also no evidence for π-π stacking interactions is found in these low energy conformations (see Figure 5). As before, the H-bonds are generally found around residues Glu11 and Asp7, though strong interactions (average length 1.526 Å over the three phen conformations) were identified between the hydroxyl group of Tyr10 and Asp7.

Conclusions

LFMM has previously been demonstrated to be a powerful tool in predicting geometries and conformations of biomolecules bound to TM species. In the present work, we aim to apply this methodology to the study of platinum-complexes of the type studied by Barnham[17,21] bound to model amyloid-β fragments in order to determine favourable metal-binding modes and peptide conformations. Thorough exploration of the conformational space of these biomolecules was achieved using LowMode MD in conjunction with AMBER molecular mechanics parameters. Comparison of calculated relative energies of a subset of these conformations indicates that LFMM fails to reproduce DFT results ($R^2 = 0.14$). However, QM evaluation of structures of this size is computationally expensive, so the less expensive semi-empirical PM7 method was utilized, which agrees well with QM results ($R^2 = 0.78$); PM7 therefore reproduces DFT energies at a much lower computational cost. In addition, PM7 optimization generally retains the DFT structure, with average all-atom RMSD of 0.817 over 158 conformers. This illustrates that PM7 accurately reproduces DFT geometries as well as energies. The present results indicate that PM7 is an appropriate and computationally manageable approach to modelling these metal-biomolecule systems.

This semi-empirical approach was subsequently extended to all conformations identified by LFMM. Statistical thermodynamics was applied to the generated databases in order to generate relative populations of each conformer at 310K. It was found that platinum coordination occurs via the Nε atom in His residues for both of the ligands investigated here. Favorable platinum-coordination modes were identified for each ligand: 6ε-13ε and 6ε-14ε for bipy and phen, respectively. Furthermore, this change in binding mode for different ligands suggests that the binding mode can be controlled by the choice of ligand.

In the bipy systems, the Boltzmann population is dominated by a single conformer that accounts for almost 80% of the weighted ensemble containing a large number of intramolecular H-bonds and a possible π-stacking interaction between His 14 and the bipy ligand. In the phenanthroline case, three conformations make significant contributions to the ensemble. Each of these conformations contains fewer intramolecular H-bonds than the dominant bipy conformation and no evidence of π-π stacking interactions was found.

As this work continues, research will focus on two areas. Firstly, the peptide fragment will be extended to at least the Aβ1-16 unit studied in experimental work[19,54]. This would allow confirmation of platinum binding modes on a more realistic model of biological Aβ. Additionally, this modelling protocol may be used to study other ligands, such as those investigated by Barnham *et al.*,[21] Collin *et al.*[55] and Yellol *et al.*[56] and Furthermore, the flexibility of LFMM allows the study of different transition metals such as those of physiological importance (*e.g.* copper and zinc)[31] or other potential therapeutics of current research interest (*e.g.* ruthenium[32] or mixed-metal complexes[57]).

Acknowledgements

This work was carried out using resources of the Advanced Research Computing @ Cardiff (ARCCA) and HPC Wales facilities. MT is grateful to Cardiff University for a studentship. RJD acknowledges the University of Edinburgh for granting an Honorary Fellowship. Molecular graphics were obtained using the UCSF Chimera package. Chimera is developed by the Resource for Biocomputing, Visualization, and Informatics at the University of California, San Francisco (supported by NIGMS P41-GM103311). RJD acknowledges the support of Chemical Computing Group.

References

(1) Brookmeyer, R.; Johnson, E.; Ziegler-Graham, K.; Arrighi, H. M. Forecasting the Global Burden of Alzheimer's Disease. *Alzheimers Dement. J. Alzheimers Assoc.* **2007**, *3*, 186–191.

(2) Valensin, D.; Gabbiani, C.; Messori, L. Metal Compounds as Inhibitors of Beta-Amyloid Aggregation. Perspectives for an Innovative Metallotherapeutics on Alzheimer's Disease. *Coord. Chem. Rev.* **2012**, *256*, 2357–2366.

(3) Elwood, P.; Galante, J.; Pickering, J.; Palmer, S.; Bayer, A.; Ben-Shlomo, Y.; Longley, M.; Gallacher, J. Healthy Lifestyles Reduce the Incidence of Chronic Diseases and Dementia: Evidence from the Caerphilly Cohort Study. *PLoS ONE* **2013**, *8*, e81877.

(4) Cai, W.; Uribarri, J.; Zhu, L.; Chen, X.; Swamy, S.; Zhao, Z.; Grosjean, F.; Simonaro, C.; Kuchel, G. A.; Schnaider-Beeri, M.; Woodward, M.; Striker, G. E.; Vlassara, H. Oral Glycotoxins Are a Modifiable Cause of Dementia and the Metabolic Syndrome in Mice and Humans. *Proc. Natl. Acad. Sci.* **2014**, 201316013.

(5) Amouyel, P. *et al.* Meta-Analysis of 74,046 Individuals Identifies 11 New Susceptibility Loci for Alzheimer's Disease. *Nat. Genet.* **2013**, *45*, 1452–U206.

(6) Masters, C.; Simms, G.; Weinman, N.; Multhaup, G.; Mcdonald, B.; Beyreuther, K. Amyloid Plaque Core Protein in Alzheimer-Disease and down Syndrome. *Proc. Natl. Acad. Sci. U. S. A.* **1985**, *82*, 4245–4249.

(7) Selkoe, D. The Molecular Pathology of Alzheimers-Disease. *Neuron* **1991**, *6*, 487–498.

(8) Walsh, D. M.; Klyubin, I.; Fadeeva, J. V.; Cullen, W. K.; Anwyl, R.; Wolfe, M. S.; Rowan, M. J.; Selkoe, D. J. Naturally Secreted Oligomers of Amyloid Beta Protein Potently Inhibit Hippocampal Long-Term Potentiation in Vivo. *Nature* **2002**, *416*, 535–539.

(9) Haass, C.; De Strooper, B. Review: Neurobiology - The Presenilins in Alzheimer's Disease - Proteolysis Holds the Key. *Science* **1999**, *286*, 916–919.

(10) Cleary, J. P.; Walsh, D. M.; Hofmeister, J. J.; Shankar, G. M.; Kuskowski, M. A.; Selkoe, D. J.; Ashe, K. H. Natural Oligomers of the Amyloid-Protein Specifically Disrupt Cognitive Function. *Nat. Neurosci.* **2005**, *8*, 79–84.

(11) Bush, A. I. The Metallobiology of Alzheimer's Disease. *Trends Neurosci.* **2003**, *26*, 207–214.

(12) Barnham, K. J.; Masters, C. L.; Bush, A. I. Neurodegenerative Diseases and Oxidative Stress. *Nat. Rev. Drug Discov.* **2004**, *3*, 205–214.
(13) Bolognin, S.; Messori, L.; Drago, D.; Gabbiani, C.; Cendron, L.; Zatta, P. Aluminum, Copper, Iron and Zinc Differentially Alter Amyloid-A beta(1-42) Aggregation and Toxicity. *Int. J. Biochem. Cell Biol.* **2011**, *43*, 877–885.
(14) Kenche, V. B.; Barnham, K. J. Alzheimer's Disease & Metals: Therapeutic Opportunities. *Br. J. Pharmacol.* **2011**, *163*, 211–219.
(15) Zirah, S.; Kozin, S. A.; Mazur, A. K.; Blond, A.; Cheminant, M.; Segalas-Milazzo, I.; Debey, P.; Rebuffat, S. Structural Changes of Region 1-16 of the Alzheimer Disease Amyloid Beta-Peptide upon Zinc Binding and in Vitro Aging. *J. Biol. Chem.* **2006**, *281*, 2151–2161.
(16) Giannozzi, P.; Jansen, K.; La Penna, G.; Minicozzi, V.; Morante, S.; Rossi, G.; Stellato, F. Zn Induced Structural Aggregation Patterns of Beta-Amyloid Peptides by First-Principle Simulations and XAS Measurements. *Metallomics* **2012**, *4*, 156–165.
(17) Barnham, K. J.; Kenche, V. B.; Ciccotosto, G. D.; Smith, D. P.; Tew, D. J.; Liu, X.; Perez, K.; Cranston, G. A.; Johanssen, T. J.; Volitakis, I.; Bush, A. I.; Masters, C. L.; White, A. R.; Smith, J. P.; Cherny, R. A.; Cappai, R. Platinum-Based Inhibitors of Amyloid-Beta as Therapeutic Agents for Alzheimer's Disease. *Proc. Natl. Acad. Sci. U. S. A.* **2008**, *105*, 6813–6818.
(18) Streltsov, V. A.; Chandana Epa, V.; James, S. A.; Churches, Q. I.; Caine, J. M.; Kenche, V. B.; Barnham, K. J. Structural Insights into the Interaction of Platinum-Based Inhibitors with the Alzheimer's Disease Amyloid-B Peptide. *Chem. Commun.* **2013**, *49*, 11364.
(19) Ma, G.; Huang, F.; Pu, X.; Jia, L.; Jiang, T.; Li, L.; Liu, Y. Identification of [PtCl2(phen)] Binding Modes in Amyloid-Beta Peptide and the Mechanism of Aggregation Inhibition. *Chem.- Eur. J.* **2011**, *17*, 11657–11666.
(20) Yao, S. G.; Cherny, R. A.; Bush, A. I.; Masters, C. L.; Barnham, K. J. Characterizing Bathocuproine Self-Association and Subsequent Binding to Alzheimer's Disease Amyloid Beta-Peptide by NMR. *J. Pept. Sci.* **2004**, *10*, 210–217.
(21) Barnham, K. J.; Kenche, V. B.; Hung, L. W.; Perez, K.; Volitakes, I.; Ciccotosto, G.; Kwok, J.; Critch, N.; Sherratt, N.; Cortes, M.; Lal, V.; Masters, C. L.; Murakami, K.; Cappai, R.; Adlard, P. A. Development of a Platinum Complex as an Anti-Amyloid Agent for the Therapy of Alzheimer's Disease. *Angew. Chem.-Int. Ed.* **2013**, *52*, 3374–3378.
(22) Robertazzi, A.; Platts, J. A. A QM/MM Study of Cisplatin-DNA Oligonucleotides: From Simple Models to Realistic Systems. *Chem.- Eur. J.* **2006**, *12*, 5747–5756.
(23) Gkionis, K.; Platts, J. A. QM/MM Investigation into Binding of Square-Planar Platinum Complexes to DNA Fragments. *JBIC J. Biol. Inorg. Chem.* **2009**, *14*, 1165–1174.
(24) Gkionis, K.; Mutter, S. T.; Platts, J. A. QM/MM Description of Platinum-DNA Interactions: Comparison of Binding and DNA Distortion of Five Drugs. *Rsc Adv.* **2013**, *3*, 4066–4073.
(25) Burton, V.; Deeth, R.; Kemp, C.; Gilbert, P. Molecular Mechanics for Coordination-Complexes - the Impact of Adding D-Electron Stabilization Energies. *J. Am. Chem. Soc.* **1995**, *117*, 8407–8415.
(26) Deeth, R. J.; Anastasi, A.; Diedrich, C.; Randell, K. Molecular Modelling for Transition Metal Complexes: Dealing with D-Electron Effects. *Coord. Chem. Rev.* **2009**, *253*, 795–816.

(27) Deeth, R. J.; Hearnshaw, L. J. A. Molecular Modelling of Jahn-Teller Distortions in Cu(II)N-6 Complexes: Elongations, Compressions and the Pathways in between. *Dalton Trans.* **2006**, 1092–1100.
(28) Deeth, R. J.; Randell, K. Ligand Field Stabilization and Activation Energies Revisited: Molecular Modeling of the Thermodynamic and Kinetic Properties of Divalent, First-Row Aqua Complexes. *Inorg. Chem.* **2008**, *47*, 7377–7388.
(29) Anastasi, A. E.; Deeth, R. J. Capturing the Trans Influence in Low-Spin d(8) Square-Planar Platinum(II) Systems Using Molecular Mechanics. *J. Chem. Theory Comput.* **2009**, *5*, 2339–2352.
(30) Tai, H.-C.; Brodbeck, R.; Kasparkova, J.; Farrer, N. J.; Brabec, V.; Sadler, P. J.; Deeth, R. J. Combined Theoretical and Computational Study of Interstrand DNA Guanine-Guanine Cross-Linking by Trans-[Pt(pyridine)(2)] Derived from the Photoactivated Prodrug Trans,trans,trans-[Pt(N-3)(2)(OH)(2)(pyridine)(2)]. *Inorg. Chem.* **2012**, *51*, 6830–6841.
(31) Maynard, C. J.; Bush, A. I.; Masters, C. L.; Cappai, R.; Li, Q. X. Metals and Amyloid-Beta in Alzheimer's Disease. *Int. J. Exp. Pathol.* **2005**, *86*, 147–159.
(32) Valensin, D.; Anzini, P.; Gaggelli, E.; Gaggelli, N.; Tamasi, G.; Cini, R.; Gabbiani, C.; Michelucci, E.; Messori, L.; Kozlowski, H.; Valensin, G. Fac-{Ru(Co)(3)}(2+) Selectively Targets the Histidine Residues of the Beta-Amyloid Peptide 1-28. Implications for New Alzheimer's Disease Treatments Based on Ruthenium Complexes. *Inorg. Chem.* **2010**, *49*, 4720–4722.
(33) *Molecular Operating Environment (MOE),(2013.08)*; Chemical Computing Group Inc.: 1010 Sherbooke St. West, Suite #910, Montreal, QC, Canada, H3A 2R7, 2013.
(34) Cornell, W.; Cieplak, P.; Bayly, C.; Gould, I.; Merz, K.; Ferguson, D.; Spellmeyer, D.; Fox, T.; Caldwell, J.; Kollman, P. A 2nd Generation Force-Field for the Simulation of Proteins, Nucleic-Acids, and Organic-Molecules. *J. Am. Chem. Soc.* **1995**, *117*, 5179–5197.
(35) Deeth, R. J.; Fey, N.; Williams–Hubbard, B. DommiMOE: An Implementation of Ligand Field Molecular Mechanics in the Molecular Operating Environment. *J. Comput. Chem.* **2005**, *26*, 123–130.
(36) Frisch, M. J.; Trucks et al., G. W. *Gaussian09*; Gaussian Inc.: Wallingford, CT, 2009.
(37) Labute, P. LowModeMD—Implicit Low-Mode Velocity Filtering Applied to Conformational Search of Macrocycles and Protein Loops. *J. Chem. Inf. Model.* **2010**, *50*, 792–800.
(38) Chen, I.-J.; Foloppe, N. Tackling the Conformational Sampling of Larger Flexible Compounds and Macrocycles in Pharmacology and Drug Discovery. *Bioorg. Med. Chem.* **2013**, *21*, 7898–7920.
(39) Kobayashi, M.; Kinjo, T.; Koseki, Y.; Bourne, C. R.; Barrow, W. W.; Aoki, S. Identification of Novel Potential Antibiotics against Staphylococcus Using Structure-Based Drug Screening Targeting Dihydrofolate Reductase. *J. Chem. Inf. Model.* **2014**, *54*, 1242–1253.
(40) Becke, A. D. Density-functional Thermochemistry. III. The Role of Exact Exchange. *J. Chem. Phys.* **1993**, *98*, 5648–5652.
(41) Fuentealba, P.; Preuss, H.; Stoll, H.; Vonszentpaly, L. A Proper Account of Core-Polarization with Pseudopotentials - Single Valence-Electron Alkali Compounds. *Chem. Phys. Lett.* **1982**, *89*, 418–422.
(42) Andrae, D.; Haussermann, U.; Dolg, M.; Stoll, H.; Preuss, H. Energy-Adjusted Abinitio Pseudopotentials for the 2nd and 3rd Row Transition-Elements. *Theor. Chim. Acta* **1990**, *77*, 123–141.

(43) Miertus, S.; Scrocco, E.; Tomasi, J. Electrostatic Interaction of a Solute with a Continuum - a Direct Utilization of Abinitio Molecular Potentials for the Prevision of Solvent Effects. *Chem. Phys.* **1981**, *55*, 117–129.
(44) Cammi, R.; Tomasi, J. Remarks on the Use of the Apparent Surface-Charges (asc) Methods in Solvation Problems - Iterative Versus Matrix-Inversion Procedures and the Renormalization of the Apparent Charges. *J. Comput. Chem.* **1995**, *16*, 1449–1458.
(45) Waller, M. P.; Robertazzi, A.; Platts, J. A.; Hibbs, D. E.; Williams, P. A. Hybrid Density Functional Theory for Π-Stacking Interactions: Application to Benzenes, Pyridines, and DNA Bases. *J. Comput. Chem.* **2006**, *27*, 491–504.
(46) Grimme, S.; Ehrlich, S.; Goerigk, L. Effect of the Damping Function in Dispersion Corrected Density Functional Theory. *J. Comput. Chem.* **2011**, *32*, 1456–1465.
(47) Zhao, Y.; Truhlar, D. G. The M06 Suite of Density Functionals for Main Group Thermochemistry, Thermochemical Kinetics, Noncovalent Interactions, Excited States, and Transition Elements: Two New Functionals and Systematic Testing of Four M06-Class Functionals and 12 Other Functionals. *Theor. Chem. Acc.* **2007**, *120*, 215–241.
(48) Stewart, J. J. P. *Http://openmopac.net/index.html*. Accessed 1st July 2015.
(49) Stewart, J. J. P. Optimization of Parameters for Semiempirical Methods VI: More Modifications to the NDDO Approximations and Re-Optimization of Parameters. *J. Mol. Model.* **2013**, *19*, 1–32.
(50) Klamt, A.; Schüürmann, G. COSMO: A New Approach to Dielectric Screening in Solvents with Explicit Expressions for the Screening Energy and Its Gradient. *J. Chem. Soc. Perkin Trans. 2* **1993**, 799–805.
(51) Pettersen, E. F.; Goddard, T. D.; Huang, C. C.; Couch, G. S.; Greenblatt, D. M.; Meng, E. C.; Ferrin, T. E. UCSF Chimera--a Visualization System for Exploratory Research and Analysis. *J. Comput. Chem.* **2004**, *25*, 1605–1612.
(52) Kabsch, W. A Solution for the Best Rotation to Relate Two Sets of Vectors. *Acta Crystallogr. Sect. A* **1976**, *32*, 922–923.
(53) Charnley, J. *GitHub: Calculate RMSD for Two XYZ Structures*. Accessed 1st September 2015
(54) Ma, G.; Wang, E.; Wei, H.; Wei, K.; Zhu, P.; Liu, Y. PtCl2(phen) Disrupts the Metal Ions Binding to Amyloid-B Peptide. *Metallomics* **2013**, *5*, 879.
(55) Collin, F.; Sasaki, I.; Eury, H.; Faller, P.; Hureau, C. Pt(II) Compounds Interplay with Cu(II) and Zn(II) Coordination to the Amyloid-Beta Peptide Has Metal Specific Consequences on Deleterious Processes Associated to Alzheimer's Disease. *Chem. Commun.* **2013**, *49*, 2130–2132.
(56) Yellol, G. S.; Yellol, J. G.; Kenche, V. B.; Liu, X. M.; Barnham, K. J.; Donaire, A.; Janiak, C.; Ruiz, J. Synthesis of 2-Pyridyl-Benzimidazole Iridium(III), Ruthenium(II), and Platinum(II) Complexes. Study of the Activity as Inhibitors of Amyloid-B Aggregation and Neurotoxicity Evaluation. *Inorg. Chem.* **2015**, *54*, 470–475.
(57) Rangachari, V.; Kumar, A.; Moody, L.; Olaivar, J. F.; Lewis, N. A.; Khade, R. L.; Holder, A. A.; Zhang, Y. Inhibition of A Beta 42 Peptide Aggregation by a Binuclear Ruthenium(II)-Platinum(II) Complex: Potential for Multimetal Organometallics as Anti-Amyloid Agents. *Acs Chem. Neurosci.* **2010**, *1*, 691–701.

ASSOCIATED CONTENT

Supporting Information. Comparison of the performance of different DFT methods against X-ray crystallographic geometry for a series of model compounds, and Cartesian coordinates for structures reported in Table 5. This material is available free of charge via the Internet at http://pubs.acs.org.

AUTHOR INFORMATION

Corresponding Author

* Dr. James A. Platts, School of Chemistry, Cardiff University, Park Place, Cardiff CF10 3AT, UK. Email: platts@cardiff.ac.uk ; Phone: +44-2920-874950

Present Addresses

† School of Chemistry, University of Edinburgh, EH9 3FJ.

Table of Contents Graphic

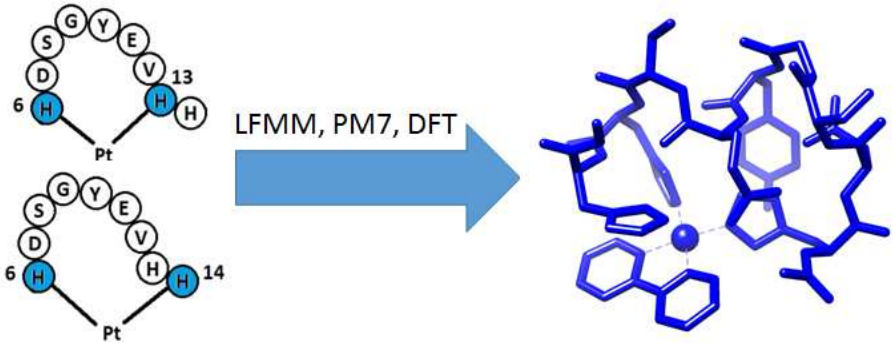

A combination of molecular mechanics, semi-empirical and DFT methods are used to predict the binding of two different platinum-aryl complexes to a fragment of the N-terminal region of amyloid-β peptide.